Wind and Structures, *Vol. 25, No. 6 (2017) 551-567*
DOI: https://doi.org/10.12989/was.2017.25.6.551

Investigations of H-Darrieus rotors for different blade parameters at low wind speeds

Anal R. Sengupta[*1], Agnimitra Biswas[2a] and Rajat Gupta[2b]

[1]*Department of Mechanical Engineering, GIMT Guwahati, Guwahati-781017, India*
[2]*Department of Mechanical Engineering, NIT Silchar, Assam-788010, India*

(Received January 4, 2017, Revised November 29, 2017, Accepted December 5, 2017)

Abstract. Studies of unsymmetrical blade H-Darrieus rotors at low wind speeds in terms of starting time, static torque, and power performances for different blade parameters: thickness-to-chord (t/c), camber position, and solidity are scarce. However these are required for knowing insights of rotor performances to obtain some design guidelines for the selection of these rotors. Here, an attempt is made to quantify the effects of these blade parameters on the performances of three different H-Darrieus rotors at various low wind streams. Different blade profiles, namely S815, EN0005 (both unsymmetrical), and NACA 0018 (symmetrical blade for comparison) are considered. The rotors are investigated rigorously in a centrifugal blower apparatus. Firstly the dynamic and static performances of the rotors are evaluated to determine the best performing rotor and their optimum solidity. Generalised performance equations are developed based on selected blade parameters which are validated for the unsymmetrical rotors. Further, the starting time is quantified with respect to the rotor inertia to determine the suitable range of inertia that helps the unsymmetrical blade rotor to self-start earlier than the symmetrical one. This study can work as a benchmark for the selection of optimum blade parameters while designing an unsymmetrical blade rotor at low wind speeds.

Keywords: blade parameters; H-Darrieus rotor; low wind speed; power coefficient; starting time; torque coefficient

1. Introduction

H-Darrieus rotors exhibited poor self-starting characteristics with symmetrical blade designs (Mohamed 2012, Errikson *et al*. 2008, Singh *et al*. 2015, Bhuyan and Biswas 2014). To overcome this various researchers performed various methods in this direction like: introducing guide-vane (Takao *et al*. 2009), using unique blade design that changes to an airfoil profile while rotating (DeCoste *et al.* 2004, Bhatta *et al.* 2008), combining Savonius with Darrieus rotor to make the latter self-starting (Gupta *et al.* 2008), engaging mechanical system to optimize the blade pitch (Paraschivoiu *et al*. 2009) etc. But all these solutions have some disadvantages like the complexity of fabrication, need of well supported blades, decrement in highest efficiencies, lower operating

*Corresponding author, Assistant Professor, E-mail: analsengupta88@gmail.com
[a] Assistant Professor, E-mail: agnibis@yahoo.co.in
[b] Professor, E-mail: rguptanitsri@gmail.com

http://www.techno-press.org/?journal=was&subpage=7 ISSN: 1226-6116 (Print), 1598-6225 (Online)

range of speed ratio etc. This speed ratio for vertical axis wind turbines varies depending on blade airfoil profile used, the number of blades, and the type of wind rotor etc. In low speed ratio, the power coefficient may be less but due to significant dynamic torque those rotors can be used in small scale applications like pumping, grinding etc. (Singh *et al.* 2015, Sengupta *et al.* 2016, Sengupta *et al*. 2017). In case of high speed ratio, power coefficient will increase, but up to a certain optimal limit for the respective rotors. Again, higher speeds result in higher noise levels which is not desirable and need stronger blades due to higher centrifugal forces. Later on unsymmetrical blades acclaimed better design prospects towards attainment of decent self-starting characteristics (Dereng, US patent 4264279). Dominy *et al*. (2007) performed an experimental study on the start-up features of H-Darrieus rotor with NACA0012 blade at wind speed of 10 m/s and concluded that, such H-Darrieus rotor having three numbers of blades is capable of self-starting when wind speed is steady. Baker (1983) compared the performances between a symmetrical and an unsymmetrical blade having NACA 0012 profile and found that the unsymmetrical blade generated higher tangential thrust for a high range of angle of attack. Of-late high solidity H-Darrieus rotors having three blades are being examined by many researchers (Singh *et al*. 2015, Bhuyan *et al*. 2014, Mohamed 2013, Deshpande and Li 2013, Saeidi *et al.* 2013). They found that for blade solidity range of 0.4-1 and in low wind speed conditions, different unsymmetrical blade H-Darrieus rotors have self-starting ability and show power coefficient in the range of 0.28-0.47. Danao *et al.* (2012) performed a numerical study of blade thickness and camber effects on the performance of three blade H-Darrieus rotor using two unsymmetrical blades namely, NACA 5522 and LS0421. It was concluded that slightly cambered blade improve the overall performance of H-Darrieus rotor and showed that LS0421 blade rotor with 2.3% camber displayed power coefficient 0.40 which is much higher than NACA5522 rotor that has 5% camber. Zamani *et al*. (2016) performed a numerical study of airfoil thickness effects on J-shaped H-rotor and found that higher thickness of such airfoil profiles leads to performance increment of such H-rotor.

From the existing literature it is seen that three-bladed H-Darrieus rotors with high solidity and unsymmetrical blades entail better prospects of both self-starting and power performances. However different unsymmetrical blades possess different thickness and camber values depending on which their performances also vary. This is because unsymmetrical blades have definite camber position, percentage camber, thickness-to-chord ratio and solidity that are characteristics of the aerodynamics of the rotors. Thus for different blade profiles, the aerodynamics and hence the performances of the rotors are also different. Further, the starting time evaluation is also quite significant since the energy yield can be increased by successfully lowering the starting time of the rotor. Studies of this parameter are not significantly available in the literature, however it could be important to improve the starting features of unsymmetrical blade H-Darrieus rotor. At this stage it is felt that some design guidelines are required for the selection of these important blade parameters so as to obtain some insights of the performances of unsymmetrical blade H-Darrieus rotors at different low wind speed conditions.

In this paper, an attempt has been made to quantify the effects of different blade parameters on the static and dynamic performances of three different H-Darrieus rotors for low wind speeds in the range 3 to 8 m/s. The Reynolds number corresponding to the wind velocities of 3 m/s, 4 m/s, 5 m/s, 6 m/s, 7 m/s and 8 m/s are 63800, 85066, 106333, 127600, 148866 and 170133. Three different blade designs, namely NACA 0018 (symmetrical), EN0005 profile (Batista *et al.* 2011) and S815 profile (both unsymmetrical) have been considered. NACA 0018 blade rotor has been chosen to make a comparison as it is widely used in case of various investigation on H-Darrieus

rotors (Batista *et al*. 2011). The performances of all the H-Darrieus rotors have been investigated rigorously in a centrifugal blower test rig. Further, starting time of the H-Darrieus rotors are also presented with respect to rotor inertia considering the blade parameters and wind speed conditions.

2. Details of the fabricated H-Darrieus rotors

To fabricate all three bladed H-Darrieus rotors, firstly the outlines of NACA 0018, EN0005 and S815 shapes are generated which can be seen in Figs. 1(a)-1(c). Then to fabricate the blades of H-rotor, wooden blocks of necessary dimensions are chosen. The coordinates of the selected airfoils are plotted on a graph and the printed shapes are pasted on both sides of the wooden block.

Then using a steel rule, lines are drawn and marked by chisel on the blocks to maintain the accuracy of the models blades. Then metal jack plane and chisel are used on the upper and lower surface of the blade respectively to remove the extra materials from the wooden block. Lastly, blades are made smooth by rubbing sand paper. Balsa wood has been chosen as the blade material because it is readily available, easily shaped and has light weight as well as enough stiffness to endure the wind thrust (Singh *et al.* 2015, Tillman 2011). Here, each of the blades have 29 cm height (H) and 5 cm chord (c) which are fixed for all the rotors. Through fully threaded circular struts, these blades are attached to a MS shaft of 1.2 cm diameter and length of 70 cm. Single struts are used so that each blade can be mounted at their mid chord locations. There are three struts joined by arc welding to the central shaft which are 120° apart from each other. Each of the struts have length of 19 cm and diameter of 4 mm. The solidity values are taken as 0.46, 0.51 and 0.56 respectively for which the aspect ratios are 0.9, 1.0 and 1.1 for the rotors. Petrol is used to clean and wash the bearings and lubricating oil is used regularly to minimize friction. Fig. 1(d) is showing the picture of the actual experimental setup**.**

Before taking readings, sufficient care was taken so that the rotors are fully open to the on-coming wind stream and there is no interference from the side columns of the supporting structure. The side columns are away from the outer diameter of the H-Darrieus rotors by 25 cm on either side. Moreover, the top surfaces of the blades are also below the beam of the supporting structure by 15 cm. So, there should not be any impact of the structural bars in the on-coming wind streams. In the given image 1(d), because of the projection (camera angle), it seems that the blades ends are very close to the supporting structure, which is not in reality. Even then, in our experimentation, the target is low wind speed conditions for which the effective swept area of the rotor in rotation will be much less for which it will not interfere with the side columns. Therefore, in any direction whether height or width, the wind streams should not interfere with the supporting structure.

The solidity (σ) of the rotors has been calculated using Eq. (1) (Singh *et al*. 2015), which can be defined as the ratio of the blades surface area to the rotor's frontal area. For each of the rotors, blade number (N) has been kept three.

$$\sigma = \frac{Nc}{D} \tag{1}$$

where D = rotor's diameter.

The blade height of 29 cm has been fixed based on the outlet dimension of the blower which is 25 cm. Now, here one of our objective is to study H-Darrieus rotor in high solidity values which

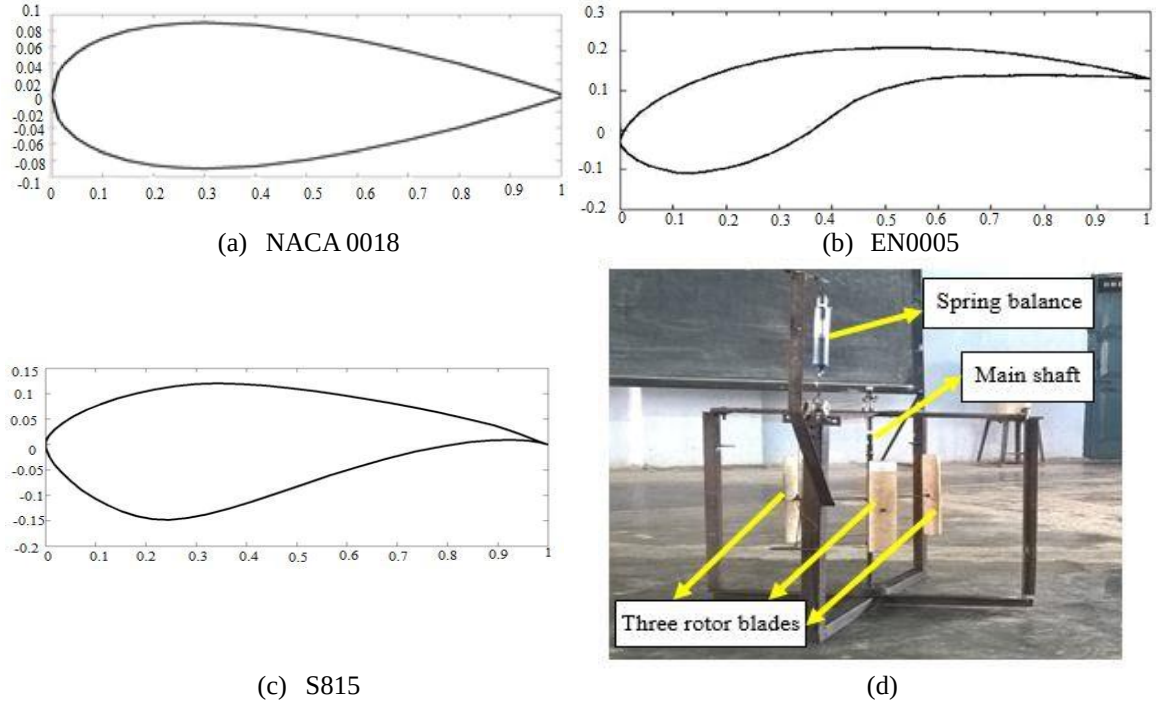

(a) NACA 0018 (b) EN0005

(c) S815 (d)

Fig 1. Outline of (a) NACA 0018 profile, (b) EN0005 profile, (c) S815 profile and (d) Actual image of the experimental setup

are considered as 0.46, 0.51 and 0.56. Now, in Eq. (2), $N = 3$ and the value of D is obtained from the H/D values (0.9, 1.0 and 1.1) corresponding to high solidity values. So, if we put the values of N, D and σ in the expression of σ, then we will get chord as 5 cm.

3. Experimental procedure

The H-Darrieus rotors along with the rotor assembly are placed in open air at the outlet of a centrifugal blower apparatus which is presented in Fig. 2(a). The blower is run by an electric motor which have 10 hp and 2800 rated rpm. By rotating the hand wheel on the blower, the wind velocity can be controlled as per requirement. The blower is measured to have turbulent intensity of not more than ±1%. The rotors positions are firstly located and finalized in the free-stream zone to obtain uniform wind velocity throughout the swept area of the rotors for all the three solidity values. Lastly, the wind speed at the mid-position of the rotors is taken for calculation. A digital vane type anemometer which ranges within 0-30 m/s and has the accuracy level of ±5%, is used to measure the wind speed. Again, a digital non-contact tachometer having accuracy level of ±1% is used to measure the rpm of the rotors. The start-up time of the rotors for various azimuthal angles are measured by a digital stopwatch having least count of 0.01 second. It has been found that the overall uncertainty (Ψ_O) of these devices as given by Eq. (2) (Singh *et al.* 2015, Bhuyan and Biswas 2014) is ±1.414%.

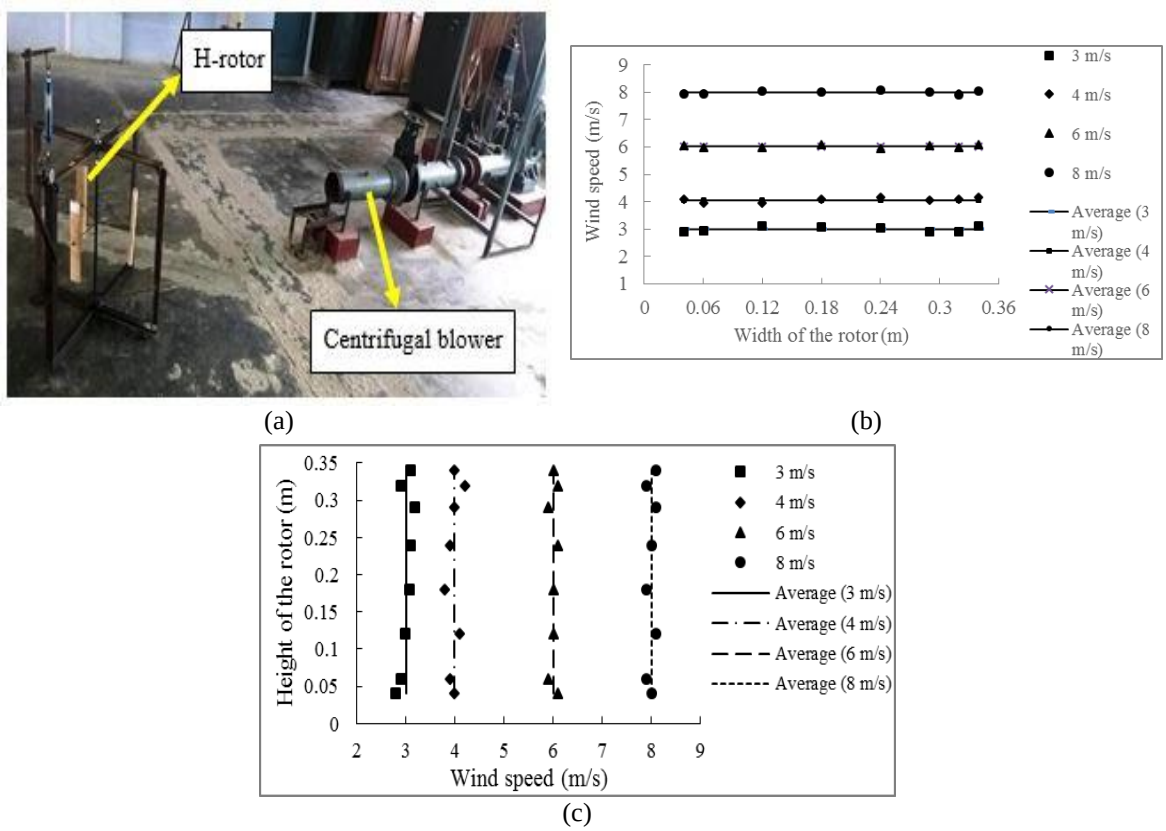

Fig.2. (a) Real image of the whole test setup, (b) wind speed variation along the width of the rotors and (c) wind speed variation along the height of the rotors

$$\psi_0 = [(\psi_{AM})^2 + (\psi_{TM})^2]^{\frac{1}{2}} \quad (2)$$

where Ψ_{AM} and Ψ_{TM} are the uncertainties in the Anemometer and Tachometer readings respectively.

The flow uniformity is ensured here which can be seen in Fig. 2(b) which shows the variation of wind velocity across the rotor width. It is seen that the deviation of the upper and lower limit values from the average wind velocity is within ±1%. Therefore these average wind velocities are considered for this current experimental analysis. Each set of experiments have been repeated up to around 4 to 5 times so that correct and precise results can be attained. For the centrifugal blower apparatus, necessary care has been taken to ensure that the required standards of experimentations are followed. When the flow emanates from the blower outlet, it is diffused. For this, the necessary insertion effects has been considered so that the rotors are placed sufficient distance away from the blower outlet in the fully developed zone where the velocity is uniform in the width direction of the rotor. Considering this, we have obtained such locations downstream the blower outlet for all test samples where the velocity distributions across the rotor width are measured and plotted in Fig. 2(b), which are found to be uniform within ± 1%.

In Fig. 2(a), the turbine setup is shown to be very close to the blower exit to show these in a

single image, but in reality the wind rotor setup was placed sufficient distance away (in the range of 2.5 m to 3.5 m for different wind speeds) from the blower exit to get the uniform velocity (for all the wind speeds considered) in the width direction as well as in the height direction of the rotor. When the wind flow comes out of the blower exit, it gets diffused in the downstream direction. If the wind rotor is placed very close to the blower exit, it will meet the diffusing flow and the upstream wind velocity might not remain uniform across the wind rotor in length and breadth directions. Hence to nullify this effect, the position of the wind turbine at the blower exit was varied to ascertain the location of uniform flow within the distance 2.5 m to 3.5 m downstream the blower exit. It was also physically ensured that the wind swept past the full width and height of the wind rotor. Further, it was cross-checked to identify whether there was any non-uniformity of wind velocity once the rotor was placed. For this, the upstream wind velocity and the variation of the same at the mid plane of the wind rotor as well as in the vertical direction was measured using the anemometer. The wind speed variation along the height of the rotors have now been plotted in Fig. 2(c). In the figure, it can be seen that the deviation of the upper and lower limit values from the average wind velocity is within acceptable range.

Here, the blade aspect ratio has been decided based on the limitation of the experimental set up.

The centrifugal blower outlet diameter is 30 cm for which the height of the rotor is selected as 29 cm. Since our objective is to study the effect of high rotor solidity, so based on our selected high solidity values, chord length from the solidity formula is found to be 5 cm. For this chord length and limited blade height, the blade aspect ratio resulted in 5.8. But, in some existing literature (Howell *et al*. 2010), they have considered low blade aspect ratio of 4 as their objective was to study the aerodynamics of small size vertical axis rotor which is also the objective of our present paper.

In comparison to that study, we have also considered unsymmetrical blade. For our present study, the objective is to improve the performance of unsymmetrical blade H-Darrieus rotor. The blade twist in unsymmetrical blade would break the wake structure (due to separation) at the blade trailing edge creating vortices. This would lessen the rigorous wake effect of the preceding blade from interfering with the succeeding blade, which happens with symmetrical blade with low aspect ratios. Further, these separating vortices rolls up the blade curvature and interacts with the blades during both power and return strokes thereby improving the performance of the rotor in low wind stream. This physics of the unsymmetrical blade rotor with low aspect ratio has also been reported in the existing literature (Biswas and Gupta 2014). The actual quantification of these tip vortices for unsymmetrical blade can be an important area of future study.

To estimate the torque of the rotors, a rope brake dynamometer arrangement is used as shown in Fig. 1(d). A nylon string is twirled around a pulley attached to the rotor shaft through which a brake load is suspended and the other end of the string is knotted to the dynamometer spring balance to determine its reading. The diameter of rope (nylon string) is 0.12 cm. Dynamometer spring balance is used to measure the torque values of rotors whose least count is 5 gms. The mechanical torque (T) produced by the rotor shaft is measured by observing the weights and the spring balance readings and later putting these data in the following Eq. (3) (Bhuyan and Biswas 2014)

$$T = (M - S) \times \left(r_{shaft} + d_s\right) \times g \tag{3}$$

where M is the load, S is the spring balance load, r_{shaft} is the radius of the rotor shaft, d_s is the nylon string diameter and g is the gravitational acceleration. Speed ratio λ, is the ratio of the blade speed to the free-stream wind speed and can be computed using the following Eq. (4) (Singh *et al*. 2015,

Bhuyan and Biswas 2014)

$$\lambda = \frac{\omega D}{2U} \tag{4}$$

where ω is the angular velocity, D is the rotor diameter and U is the free-stream wind velocity. The performances of the rotors are calculated by finding the torque and power coefficients that can be found from the following Eqs. (5) and (6) (Singh *et al*. 2015, Bhuyan and Biswas 2014)

$$C_t = \frac{4T}{\rho U^2 D^2 H} \tag{5}$$

$$C_p = \lambda \times C_t \tag{6}$$

where ρ is the density of air, C_t is the torque coefficient and C_p is the power coefficient.

A sample reading table for dynamic torque of S815 rotor for wind speed of 6 m/s is given here in a Table 1.

3.1 Error analysis

Most of the experimental works have some unavoidable uncertainties. After finding the uncertainty calculations of Anemometer and Tachometer, now the power coefficient and torque uncertainties can be evaluated by Eqs. (7) and (8). By using the uncertainty method of Kline and McClintock (Singh *et al*. 2015, Kline and McClintock 1953), these errors can be evaluated.

$$\frac{\delta C_p}{C_p} = \sqrt{\left(\frac{\delta\omega}{\omega}\right)^2 + \left(\frac{\delta U}{U}\right)^2 + \left(\frac{\delta T}{T}\right)^2 + \left(2\frac{\delta U}{U}\right)^2} \tag{7}$$

where torque uncertainty can be calculated as

$$\frac{\delta T}{T} = \frac{\delta S}{S} \tag{8}$$

Table 1 Sample reading table for dynamic torque of S815 rotor for 6 m/s wind speed

Wind speed	Load given (gms.)	Spring balance reading (gms.)	rpm of rotor (averaged)
6 m/s	60	20	964
	100	40	900
	150	70	802
	200	95	685

4. Results and discussions

This section represents the results achieved from the experimentation of the wind rotors. But before going through that, power loss of the rotors due to different parameters need to be found out. Here the power loss of the rotors due to bearing friction and parasitic drag of struts have been plotted with respect to rpm of the rotors as shown in Fig. 3. The graph shows the average range of power loss which is almost same for all the three rotors. It has been observed that bearing power loss is higher than struts parasitic drag loss for the rotors within the operating range selected but both are less than 0.03 W. Here, the maximum loss of power due to parasitic drag of the supporting struts and due to the bearing friction is 0.04 W, which is only 1.75% of the peak power generated by this small sized vertical axis H-Darrieus rotor.

The formulae for power loss due to the bearings and struts are:

Bearing power loss = $1.05 \times 10^{-4} \times M_1 \times n$

Power loss of struts = $0.125 \times C_{d_{min}} \times \rho_{actual} \times c_1 \times \omega \times n' \times \left(\omega^2 {R_1}^4 + {U_2}^2 {R_1}^2\right)$

Figs. 4(a)-4(c) show the variation of dynamic torque coefficient with wind velocity for the rotors at selected solidities. It can be seen that for the rotors, the dynamic torque is highest for solidity 0.51 and lowest for solidity 0.46 and S815 blade rotor has higher dynamic torque than the other two rotors. The highest dynamic torque can be seen in case of S815 at solidity 0.51 when wind velocity is 6 m/s. It can also be seen that the average value of dynamic torque also has been increased in case of unsymmetrical S815 rotor.

Fig. 5 displays the variation of power coefficient (C_p) with respect to wind velocity for all the rotors at solidity 0.51. For 3 m/s wind speed, the rotors show very less C_p because at 3 m/s wind speed the rotors start rotating but when some load is applied the rotational speed decreases significantly. So 3 m/s wind speed has been considered as the lower limit of wind speed for the rotors. The power coefficient has been plotted for 0.51 solidity because in this solidity all the rotors show highest dynamic torque. From the graphs, it can be seen that, C_p values of the rotors firstly increase as speed ratio increases up to some limit, but after that it fall down with further increase of speed ratio.

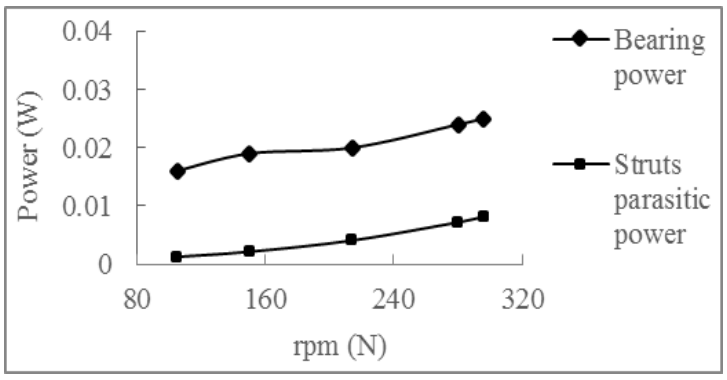

Fig. 3 Power loss due to bearing friction and struts parasitic drag

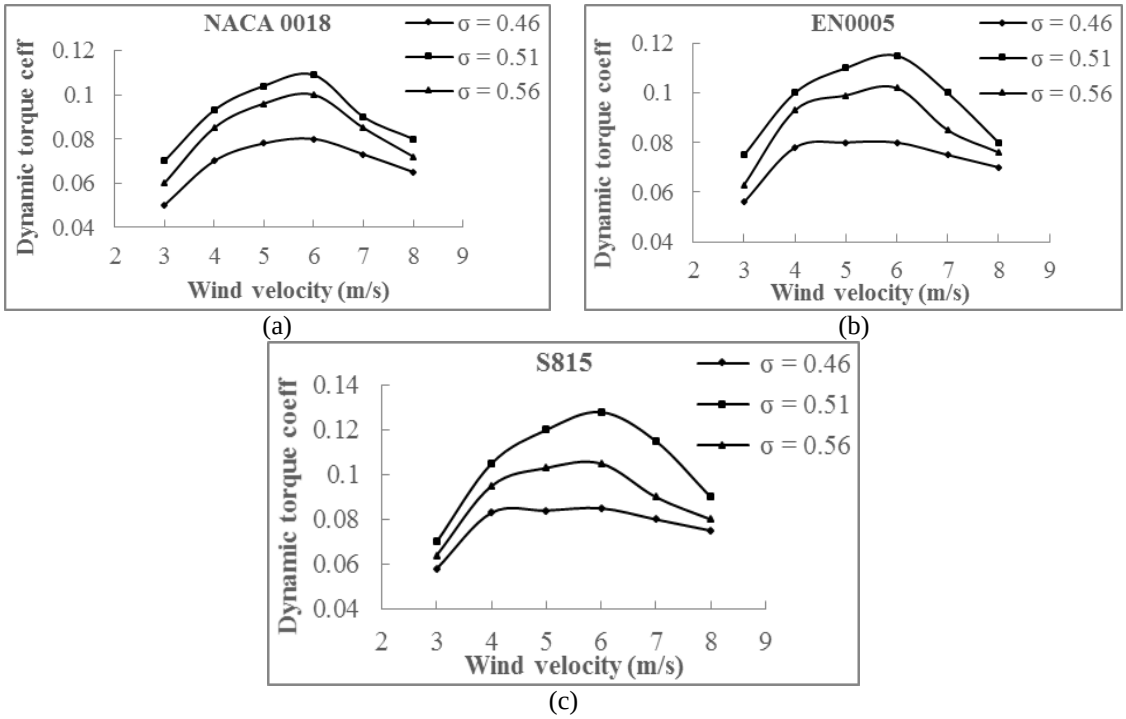

Fig. 4 Dynamic torque coefficient vs. wind velocity for (a) NACA 0018 rotor, (b) EN0005 rotor and (c) S815 rotor at different solidities

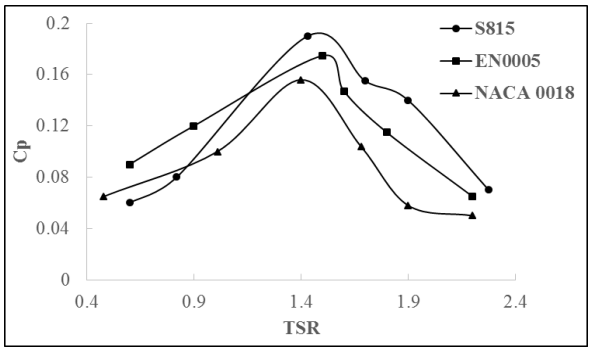

Fig. 5 Power coefficient vs. SR for (a) NACA 0018, (b) EN0005 and (c) S815 rotors at solidity 0.51

This means an optimum value of speed ratio can be found for which C_p is found to be the maximum within this wind speed range. The speed ratio values for the three rotors are in the range of 0.5 to 2.4. Here the wind velocities considered for the rotors are equal but the power coefficient (C_p) of unsymmetrical S815 rotor has been obtained higher than EN0005 and NACA 0018 rotors. In case of S815 rotor, the maximum C_p of 0.19 has been obtained at speed ratio 1.43 whereas for EN0005 and NACA 0018 rotor maximum C_p of 0.175 and 0.156 has been obtained at speed ratios of 1.5 and 1.4. In this present study the operating range of speed ratio (0.5- 2.4) is lower, as low wind speed

conditions for scaled down wind rotor models have been considered. But within this range of speed ratio, optimal value has been found for all the three selected rotors. The uncertainty in power coefficient as calculated using Eq. (7) is in 2.2% - 5.5% range and the same using Eq. (8) for torque lies in the range of 0.3% - 0.6%.

From the Fig. 5 it can be seen that the maximum power (C_p) of S815 rotor is highest compared to NACA 0018 and EN0005 rotors. This is due to the fact that, S815 unsymmetrical airfoil exhibits higher tangential thrust which helps it to offer better self-starting features and higher lift force than the other two rotors considered (Sengupta *et al*. 2016). Further, according to the study of Danao *et al.* (2012), it was concluded that slightly cambered and thick airfoil is capable of increasing the overall performance of an H-Darrieus rotor. Airfoil blade having small camber along the blade path causes the blades to generate high values of torque in both the upwind and the downwind regions which leads to higher performance of that specific rotor. Now, in this present study, S815 blade rotor has the highest thickness and least cambered among the three rotors considered which leads to exhibit the higher performance of this S815 blade rotor. For these reasons the S815 blade rotor exhibits higher power compared to the rest in the same operating range of speed ratio.

The experiment has also been performed at wind velocity of 7 m/s for S815 H-rotor to check its performance. From the Fig. 6 it can be seen that, for wind speed of 7 m/s, the peak C_p value is lower than the same of 6 m/s wind speed. It can also be seen that the highest C_p value of 8 m/s is lower compared to that at 7 m/s velocity i.e., the peak C_p value, after 6 m/s wind speed is consistently decreasing for 7 m/s and 8 m/s wind speeds. Looking at this trend, experiments were not conducted at wind speed of 9 m/s.

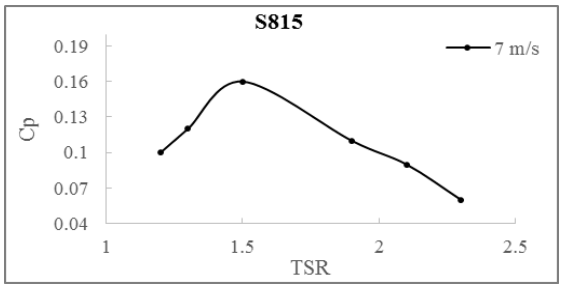

Fig. 6 Power coefficient vs. SR for S815 H-Darrieus rotor at solidity 0.51 and 7 m/s wind speed

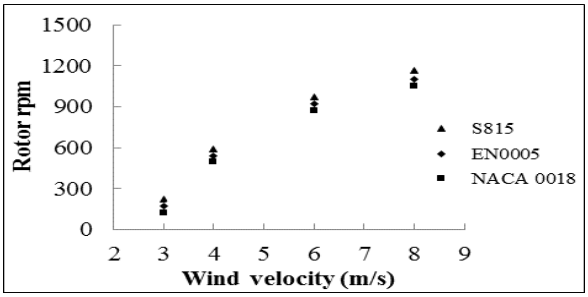

Fig. 7 Rotor rpm vs. wind velocity for all three rotors

As the rotor rpm increases from 3 to 6 m/s wind speed, its performance also increases because speed ratio (SR) increases and hence the C_p increases up to a certain limit of SR after which it decreases. In Fig. 5 it can be seen that after an optimal SR value, the C_p value decreases. The reason for decrease of C_p value after 6 m/s wind speed could be the following-

By increasing the SR value after the optimal value, the incidence angle of the relative velocity on the airfoil become smaller and then the power extraction become lower too due to lower lift coefficient.

Again, the peak performance of rotor depends not only on wind velocity, but also on rotor rpm. It is already established in literature that after an optimal SR value, C_p decreases (Singh *et al.* 2015) which is similar to the present case. Here, the Reynolds number increases with the increase of wind velocity but the dimensions of the blades are same for all the cases. With increase in velocity the rotor rpm should also sufficiently increase to increase the power coefficient. But from the Fig. 7 it can be seen that the rate of increment of rotor rpm from 4 m/s to 6 m/s wind speed is higher compared to the increment rate of rotor rpm from 6 m/s to 8 m/s case. For this reason the rotor is not able to extract sufficient energy with the high Reynolds number flow since its size is same as the previous wind velocity. So the torque as well as the lift and power coefficient decreases with high Reynolds number flow for the present small size rotor.

For finding out the self-starting ability of the three rotors, measurements of the static torque coefficients at different rotor angles were taken over a complete rotation cycle for three different rotor solidities and at wind speed 6 m/s.

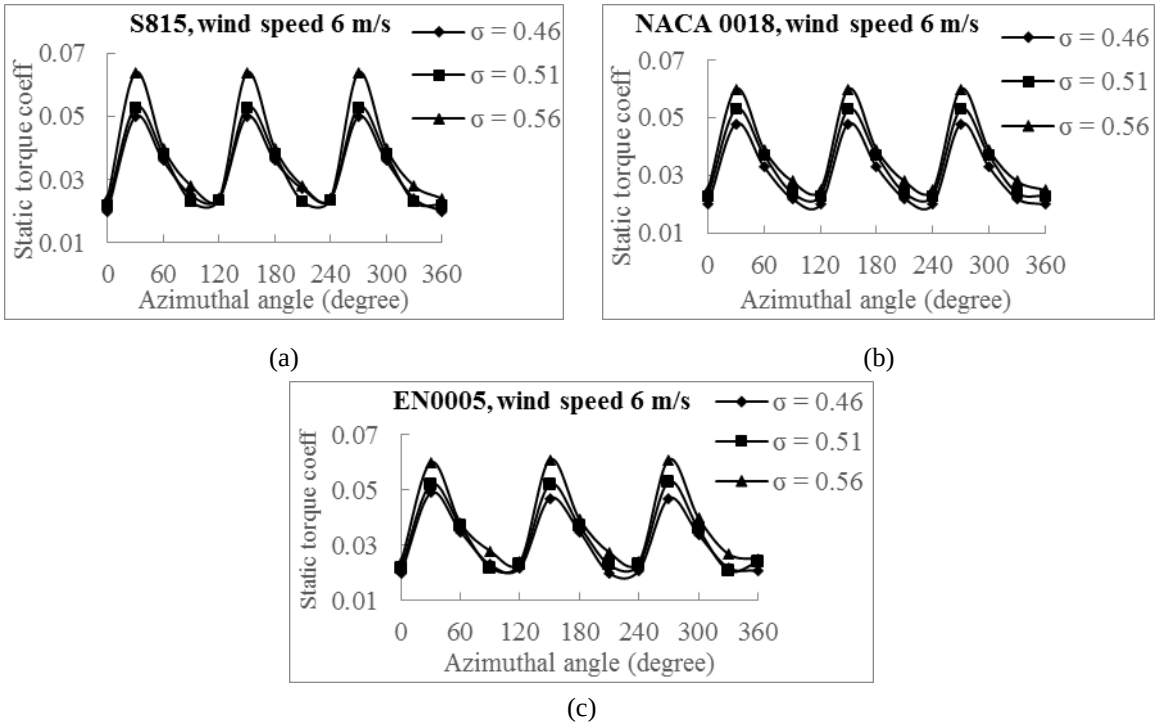

Fig. 8. Static torque coefficient vs. azimuthal angle positions of the rotors at three different solidities.

As the rotors show highest power coefficient at 6 m/s wind speed, so the graphs have been plotted for wind speed 6 m/s in Fig. 8. It can be noticed that for all the graphs the static torque values are cyclic with a periodicity of around 120° for these three blade rotors. From the graphs it can also be observed that the rotors have self-starting capability for 6 m/s wind velocity and at all the three solidities, as they show positive static torque coefficients for all rotor angular positions. It can be noticed that irrespective of wind speed condition, these static torque coefficients increase as the rotors solidity increases i.e. increased solidity leads to improved self-starting capability during starting of the rotors.

4.1 Methodology for finding performance equations:

The blade parameters that have been considered here are (t/c) ratio and camber percentage. For the considered solidities, the (t/c) ratios have been calculated for the unsymmetrical blade rotors against maximum camber percentage. As NACA 0018 is a symmetrical airfoil, so it has no camber and for the other blades the maximum percentage camber has been calculated using the following formula written as Eq. (9) [www.skf.com]

$$\text{Maximum percentage camber} = (100 \times \delta)/c \tag{9}$$

where δ = maximum distance from chord line to camber line

Using this formula maximum camber percentage is found to be 10% at 55% chord from leading edge for EN0005 blade profile. In case of S815 blade, maximum camber is 2.9% at 77.9% chord [www.dept.aoe.vt.edu]. Now the (t/c) ratios are estimated for EN0005 blade at 0.5, 0.53, 0.55 and 0.6 chords from leading edge which are found to be 0.11, 0.1, 0.098 and 0.08 respectively. For S815 blade, the (t/c) ratios are estimated for 0.73, 0.74, 0.75 and 0.779 chords from leading edge which are obtained as 0.11, 0.1, 0.098 and 0.08 i.e. the (t/c) ratio's range has been kept constant for the unsymmetrical rotors. These (t/c) ratios have been selected at that chord value for which maximum camber percentage is obtained and also at those chord values for which camber percentage is closest to the maximum value. The thickness (t) of the blade profiles have been determined by plotting the outline, and the blade chord (c) is 5 cm, which is kept constant for all rotor blades. These (t/c) ratios are considered for 0.46, 0.51 and 0.56 solidities. The (t/c) ratios corresponding to the position of maximum camber percentage and those around that position are shown in Table 2 for the two unsymmetrical blades. Usually the maximum values of the (t/c) ratio and camber position are chosen as the representative data for a specific airfoil. So, here along with the maximum values for these two parameters, the nearest to that maximum values are also taken to select the (t/c) ratio's range for the respective chord values from the leading edge of the unsymmetrical blades.

Table 2 Values of (t/c) ratios considered for the two unsymmetrical blades

(t/c) ratio	Position of camber from leading edge of the blades	
	EN0005	S815
0.11	0.50 c	0.73 c
0.10	0.53 c	0.74 c
0.098	0.55 c	0.75 c
0.08	0.60 c	0.779 c

Now as NACA 0018 is a symmetrical profile, so it has no camber and its maximum thickness is 18% at 30% chord. For S815 blade maximum thickness is 26.2% at 25.7% chord [23]. But in case of EN0005, it is an unsymmetrical profile and its maximum thickness is found 24% at 25% chord which has been calculated using the following formula presented as Eq. (10) (www.skf.com)

$$\text{Maximum percentage thickness} = (100 \times t)/c \tag{10}$$

where t = maximum distance between the upper and lower surface of the airfoil.

By regression analysis in MS Excel software, some equations have been generated for the optimum condition for which the C_p is maximum and corresponding to that the required speed ratios, (t/c) ratios and camber positions have been considered and the equations are as follows:

For EN0005

$$(t/c) = 0.076 + (0.025 \times \text{speed ratio}) - (0.055 \times C_p) \tag{11}$$

$$\text{Camber position} = 0.482 + (0.127 \times \text{speed ratio}) - (0.66 \times C_p) \tag{12}$$

For S815

$$(t/c) = 0.075 + (0.016 \times \text{speed ratio}) + (0.011 \times C_p) \tag{13}$$

$$\text{Camber position} = 0.725 - (0.019 \times \text{speed ratio}) + (0.42 \times C_p) \tag{14}$$

The equations Eqs. (11)-(14) clearly show that there is a dependency of C_p not only on wind velocity but also on the blade profiles. The above equations are valid for the wind speed range of 3-8 m/s and speed ratio range of 0.5-2.4 which have been considered here. If the performances of these unsymmetrical blade rotors are to be enhanced then for any wind speed, the optimum blade profiles are to be decided first then the results of C_p are to be obtained like the way as obtained for EN0005 and S815 blade H-Darrieus rotors. If these unsymmetrical EN0005 and S815 rotors are to be further modified, then their thickness to chord ratio (t/c), percentage and location of camber should be known.

This gives an idea about what should be the (t/c) ratio, camber position and their optimum range for the solidity and considered wind speed range.

The (t/c) range (0.08 – 0.11) has been selected based on the maximum percentage camber and maximum percentage thickness values of the selected unsymmetrical blades. So, in this range of (t/c), the data points of C_p corresponding to various SR values are obtained from the experimental investigation and these have been validated with the regression equations. After proper fitting of the points, we have got a parabolic trend of the data points corresponding to the regression analysis values. Now, the regression analysis is based on around 50 data points of speed ratios and C_p, which have been found experimentally for the considered wind speeds. From these data points, the generalized performance equations have been obtained, which have been analysed in the form of graphical representations, where the dependencies of (t/c) can be easily observed along with its influence on the C_p values.

In Fig. 9 the variation of C_p of the two unsymmetrical rotors have been plotted for different speed ratios with respect to (t/c) values and camber positions for the solidity value 0.51. Here the (t/c) ratios and camber positions have been calculated from the generated equations and the C_p values are taken from the experimental data which have been found against respective wind speed and several other speed ratios. From the Fig. 9(a) it can be seen that most of the C_p values lie within the considered (t/c) ratio's range (0.08-0.11). From the Fig. 9(b) it can be observed that most of the C_p values also lie within the considered camber position values range for the two rotors respectively. In the above Figs., the trendlines also have been drawn for the C_p values corresponding to $\sigma = 0.51$. It can be observed

that polynomial (order 2) curves are the suitable trendline curves fitting the rotors for which the value of coefficient of determination (R^2) is in the range of 0.82- 0.90.

In Fig. 10(a) variation of C_p vs. (t/c) ratio has been plotted for three different blade profiles form published results which reveal that most of the C_p values generated using Eq. (13), lie within our considered (t/c) range. Some of the C_p values for S818 falls outside our measured range which is due to the considered solidity 1.0 and speed ratios range of (2-3.8) of S818 rotor that is higher than the present study. In Fig. 10(b) the variation of C_p vs. camber position also has been plotted for the same blade profiles which shows that most of the C_p values, generated using eqn. 14, lie within our considered camber position range. Some C_p values for S1210 lie outside our selected range that is because of its higher solidity which is 1.0. In the above diagrams., the trendlines also have been drawn for the C_p values and it can be noticed that polynomial (order 2) curves are the proper trendline curves fitting the rotors for which the value of coefficient of determination (R^2) is in the range of 0.70- 0.99. So it can be said that the results have been well validated within the selected range of (t/c) and camber position within which the highest C_p have also been obtained.

This also gives us an idea about the (t/c) ratio and maximum camber position range of the unsymmetrical blades for other design conditions. If such unsymmetrical blades are to be further modified compared to this present study, then this can lead future researchers to the way of obtaining improved power coefficient by improving the operating range.

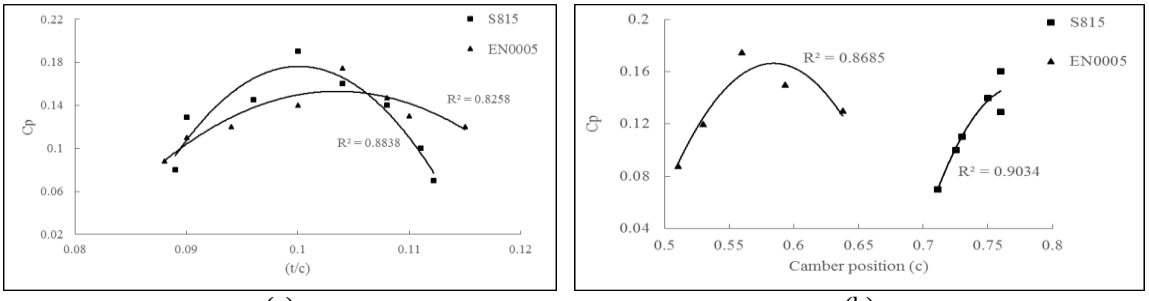

(a) (b)

Fig. 9 Variation of C_p vs. (t/c) ratio for (a) EN0005 and S815 blade rotors; C_p vs. camber position for (b) EN0005 and S815 blade rotors for solidity 0.51

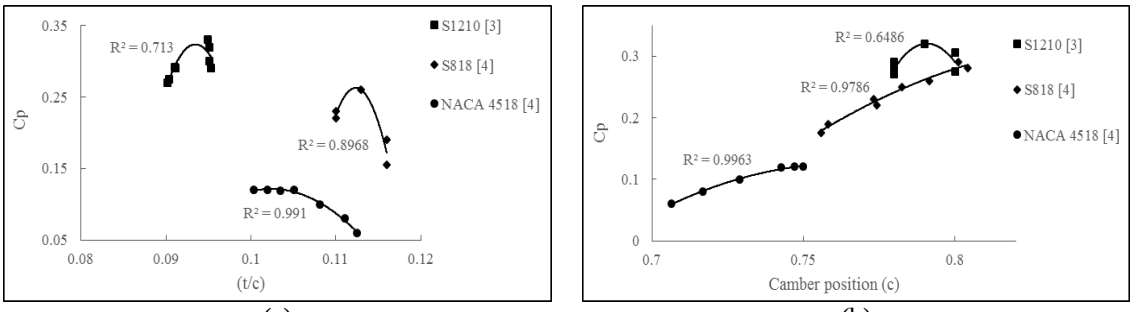

(a) (b)

Fig. 10 Variation of (a) C_p vs. (t/c) ratio and (b) C_p vs. camber position for different blade shapes

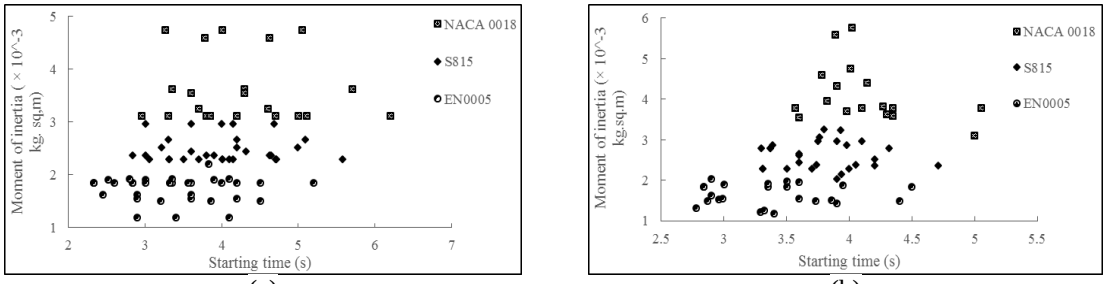

(a) (b)

Fig. 11 Moment of inertia vs. starting time for the three rotors at (a) selected wind velocities keeping solidity (σ = 0.51) constant and (b) selected rotor solidities keeping velocity (6 m/s) constant

Now, the minimum starting time of the H-Darrieus rotors for solidity value 0.51 is measured for 4 m/s, 6 m/s and 8 m/s wind velocities. As for 3 m/s wind velocity all the rotors do not show the ability to self-start at all rotor angles for all solidities considered, so the starting time measurement for 3 m/s wind speed has been excluded here. The minimum time needed for the H-Darrieus rotors for starting a steady rotation for the particular wind velocities is the starting time i.e., the least time required to generate necessary torque as the rotor completes a single full rotation. After this, the blade speed of the rotor steadily goes on increasing to its rated condition. Along with the increase in wind velocity from 4 m/s to 8 m/s, there is a reduction of the starting time of the rotors.

In Fig. 11 moment of inertia (MI) vs. starting time for all the three rotors have been drawn as the start-up time of the rotors is significantly related with respect to their inertia. Here the value of MI is calculated based on the equation given by Zhuga *et al.* (2014). In the Fig. 11(a) the starting time has been considered for 4 m/s, 6 m/s and 8 m/s wind speeds keeping σ = 0.51 constant as for this solidity the rotors show highest efficiency. In Fig. 11(b) the starting time has been considered for solidity values 0.46, 0.51 and 0.56 and keeping 6 m/s wind speed constant as for this wind speed the rotors show highest efficiency. The three different scatter points zones of inertia values for the three rotors mark the influence of inertia values on starting time. Here the group of points are generated for different wind velocities, different solidities, different azimuthal angle positions and different shapes of the blades. The cluster of points demonstrate that lower rotor inertia of EN0005 blade at the selected solidity and wind speed conditions is helping it to self-start within shortest time compared to the other rotors. This result may be helpful for future researchers to optimize the rotor blade parameters within low rotor inertia level at the present solidity and wind speed conditions, and by doing so the starting time can be minimized.

5. Conclusions

In this paper, a comprehensive study has been performed to make a quantification of different blade parameters on the static and dynamic performances of three different H-Darrieus rotors for low wind speeds in the range 3 to 8 m/s. Different blade parameters like (t/c) ratios, camber position have been studied for three different blade designs namely NACA 0018, EN0005 and S815 profile. Further, start-up time of the rotors are also investigated in some details. From this study the conclusions which can be drawn are as follows:

- S815 blade rotor has the highest dynamic torque compared to EN0005 and NACA 0018 rotors for the selected solidity and wind speed conditions.
- Optimum rotor solidity has been found 0.51 and in this solidity all the three rotors exhibit highest power coefficient, and the maximum values of power coefficient are 0.19, 0.175 and 0.156 for S815, EN0005 and NACA 0018 blade H-Darrieus rotors for speed ratios of 1.43, 1.5 and 1.4 respectively. An increase of 21.7% and 12.1% of power coefficients are obtained for S815 and EN0005 rotors respectively compared to NACA 0018 rotor.
- All the three H-Darrieus rotors display positive static torque coefficients signify that the rotors have self-starting features at the selected solidity and low wind speed condition.
- Generalized equations involving the blade parameters like (t/c) ratio and camber position have been developed for ascertaining the performances of unsymmetrical blade rotors, which are validated using published results of other different unsymmetrical blade H-Darrieus rotors.
- Lower rotor inertia of EN0005 blade at the selected solidity and wind speed conditions is helping it to self-start within shortest time compared to the other rotors. This result may be helpful for future researchers to optimize the rotor blade parameters within low rotor inertia level at the present solidity and wind speed conditions.

Finally the present research quantities the effects of important blade parameters, viz thickness-to-chord, camber position and solidity on the performances of different unsymmetrical blade H-Darrieus rotors, which would work as a benchmark for the selection of the optimum range of these blade parameters within which the unsymmetrical blade H-Darrieus rotors may be designed so as to obtain good overall performance of these rotors at low wind streams.

References

Baker, J.R. (1983), "Features to aid or enable self-starting of fixed pitch low solidity vertical axis wind turbines", *J. Wind Eng. Ind. Aerod.*, **15**, 369-380.

Batista, N.C., Melicio , R., Matias, J.C.O. and Catalao, J.P.S. (2011), "New blade profile for Darrieus wind turbines capable to self-start", *IET Conference on Renewable Power Generation*, 1-5.

Bhatta, P., Paluszek, M.A. and Mueller, J.B. (2008)," Individual blade pitch and camber control for vertical axis wind turbines", WWEC2008, Kingston, Canada.

Bhuyan, S. and Biswas, A. (2014), "Investigations on self-starting and performance characteristics of simple H and hybrid H-Savonius vertical axis wind rotors", *Energ. Convers.Manag.*, **87**, 859-67.

Biswas, A. and Gupta, R. (2014), "Unsteady aerodynamics of a twist bladed H-Darrieus rotor in low Reynolds number flow", *J. Renew. Sust. Energ.*, **6**(3), 033108.

Danao, L.A., Qin, N. and Howell, R. (2012), "A numerical study of blade thickness and camber effects on vertical axis wind turbines", *J. Power Energ.*, **226**(7), 867-881.

DeCoste, J., Smith, A., White, D., Berkvens, D. and Crawford, J. (2004), "Self-starting Darrieus wind turbine, design project mech", 4020. Dalhousie University, Hallifax, Canada,

Dereng, V.G. (1981), Fixed geometry self-starting transverse axis wind turbine, United States Patent 4264279. Available at: http://www.freepatentsonline.com/4264279.html [accessed on 29.05.15].

Deshpande, P. and Li, X. (2013), "Numerical study of giromill-type wind turbines with symmetrical and non-symmetrical airfoils", *Eur. Int. J. Sci. Technol.*, **2**(8), 195-208.

Dominy, R., Lunt, P., Bickerdyke, A. and Dominy, J. (2007), "Self-starting capability of a Darrieus turbine", *Proc. Of the I Mech E part A: J. Power Energy*, **221**(1), 111-120.

Errikson, S., Bernhoff, H. and Leijon, M. (2008), "Evaluation of different turbine concepts for wind power", *Renew. Sust. Energ.Rev.*, **12**(5), 1419-1434.

Gupta, R., Biswas, A. and Sharma, K.K. (2008), "Comparative study of a three-bucket Savonius rotor with a

combined three-bucket Savonius-three-bladed Darrieus rotor", *Renew. Energ.*, **33**(9), 1974-1981.
Howell, R., Qin, N., Edwards, J. and Durrani, N. (2010), "Wind tunnel and numerical study of a small vertical axis wind turbine", *Renew. Energ.*, **35**, 412-422.
Kline, S.J. and McClintock, F.A. (1953), "Describing uncertainties in single-sample experiments", *Mech. Eng.*, **75**(1), 3-8.
http://www.skf.com/in/products/bearings-units-housings/ball-bearings/principles/friction/power-loss-bearing-temperature/index.html (Accessed on 11/07/2016).
www.dept.aoe.vt.edu/~lutze/AOE3104/airfoilwings.pdf (Accessed on 02/09/2015).
http://airfoiltools.com/airfoil/details?airfoil=s815-nr (Accessed on 01/09/2015).
Mohamed, M.H. (2013), "Impacts of solidity and hybrid system in small wind turbines performance", *Energy*, **57**, 495-504.
Mohamed, M.H. (2012), "Performance investigation of H-rotor Darrieus turbine with new airfoil shapes", *Energy*, **47**(1), 522-530.
Paraschivoiu, I., Trifu, O. and Saeed, F. (2009), "H-Darrieus wind turbine with blade pitch control", *Int. J. Rotating Machinery*, 1-7.
Saeidi, D., Sedaghat, A., Alamdari, P. and Alemrajabi, A.A. (2013), "Aerodynamic design and economical evaluation of site specific small vertical axis wind turbines", *Appl. Energ.*, **101**, 765-775.
Sengupta, A.R., Biswas, A. and Gupta, R. (2016), "Studies of some high solidity symmetrical and unsymmetrical blade H-Darrieus rotors with respect to starting characteristics, dynamic performances and flow physics in low wind streams", *Renew. Energy* , (93), 536-547.
Sengupta, A.R., Biswas, A. and Gupta, R. (2017), "The aerodynamics of high solidity unsymmetrical and symmetrical blade H-Darrieus rotors in low wind speed conditions", *J. Renew. Sust. Energ.*, **9**, 043307.
Singh, M.A., Biswas, A. and Misra, R.D. (2015), "Investigation of self-starting and high rotor solidity on the performance of a three S1210 blade H-type Darrieus rotor", *Renew. Energ.*, **76**, 381-387.
Takao, M., Kuma, H., Maeda, T., Kamada, Y., Oki, M. and Minoda A. (2009), "A straight-bladed vertical axis wind turbine with a directed guide vane row-effect of guide vane geometry on the performance", *J. Therm. Sci.*, **18**(1), 54-57.
Tillman, J.P. (2011), "Improvements to vertical axis wind turbine blades to aid in self-starting", Masters Theses. Paper 697, http://thekeep.eiu.edu/theses/697 (Accessed on 02/09/2015).
Zamani, M., Maghrebi, M.J. and Moshizi, S.A. (2016), "Numerical study of airfoil thickness effects on the performance of J-shaped straight blade vertical axis wind turbine", *Wind Struct.*, **22**(5), 595-616.
Zhuga, A.T., Munyaradzi, B. and Shonhiwa, C. (2014), "Design of Alternative Energy Systems: A Self-Starting Vertical Axis Wind Turbine for Stand-Alone Applications (charging batteries)", *Proceedings of the 6th International Conference on Appropriate Technology*.

CC